Supporting Information

Anion Recognition-Triggered Nanoribbon-Like Self-Assembly: A Novel Fluorescent Chemosensor for NO_3^- in Acidic Aqueous Solution and Living Cells

Yaping Yang, Shiyan Chen and Xin-Long Ni*

Key Laboratory of Macrocyclic and Supramolecular Chemistry of Guizhou Province, Guizhou University, Guiyang 550025, China

E-mail: longni333@163.com

Synthesis of 1-6

Scheme S1.

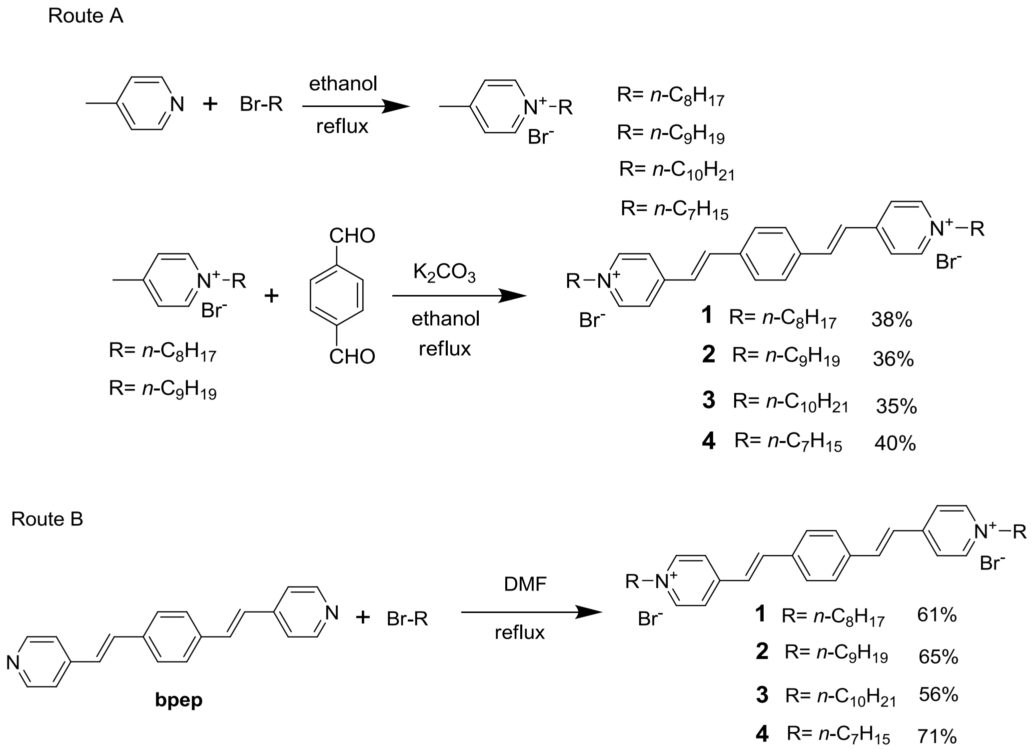

Scheme S2.

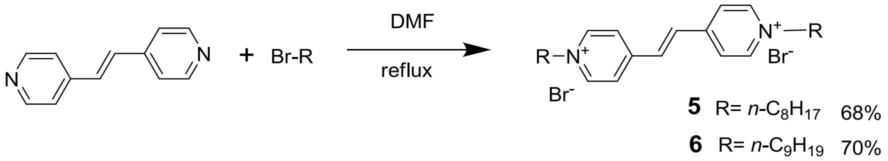

Synthesis of **1-4**.

Route A. we first synthesis of the compound **1-4** according to the reported literature.[1] For example, a mixture of Br-C_8H_{17} (770 mg, 4 mmol) and 4-picoline (560 mg, 6 mmol) in ethanol (10 mL) and was heated to reflux for 24 hours to obtain the corresponding 4-picolinium salt. Then the reaction mixture was cooled and an excess amount of 4-picoline was removed under vacuum followed by repeated washing with petroleum ether to give rise to a white solid. The 4-picolinium salt (860 mg, 3 mmol) and 1,4-Phthalaldehyde (200 mg, 1.45 mmol) were then dissolved in 20 mL ethanol, and an aqueous solution (0.5 mL) of 5 M NaOH was added dropwise into the ethanol solution under ice-cold conditions. The mixture was stirred under ice cold conditions for 4 hours, and then the reaction was quenched by acidification with 4M HCl. The precipitate was filtered and washed with ice-cold water. The crude product was dissolved in small amount of methanol and precipitated in ethyl acetate, followed by filtration and washed with ice-cold water again to obtain a yellow solid 210 mg (yield 21.6%).

Route B. A mixture of **bpep**[2] (285 mg, 1.0 mmol) and Br-C_8H_{17} (580 mg, 3.0 mmol) in DMF was refluxed for 48 hours. The resulting precipitate was filtered and washed with DMF and petroleum ether, and then dried under vacuum to obtain a yellow solid 410 mg (yield 61%).

Compared to **Route A**., the modified synthetic **Route B**. is of simple experiment operation and higher yield for the target compounds, therefore, a similar method as **Route B** was used to prepare compounds **2-6**.

Characterizations of **1-6**

1: ^{1}H NMR (500MHz, DMSO-$_{d6}$), δ 8.97-8.96 (d, *J* =5 Hz, 4H, Ar-H), 8.25-8.23 (d, *J* =10 Hz, 4H, Ar-H), 8.06-8.03 (d, *J* =15 Hz, 2H, vinyl-H), 7.84 (s, 4H, Ar-H), 7.63-7.60 (d, *J* =15 Hz, 2H, vinyl-H), 4.49-4.46 (t, 4H, N^{+}-CH_2), 1.89-1.86 (t, 4H, CH_2), 1.26-1.21 (m, 20H, CH_2), 0.85-0.82 (t, 6H, CH_3). ^{13}C NMR (100 MHz, CD_3OD): 155.12, 145.34, 141.78, 138.59, 130.10, 125.55, 125.27, 62.01, 32.89, 32.35, 30.21, 30.11, 27.23, 23.68, 14.42. MALDI-TOF: m/z calcd for $C_{36}H_{50}N_2^{2+}$: 510.79; found: 511.156; elemental analysis calcd (%) for $C_{36}H_{50}N_2Br_2$: C 64.48, H 7.52, N 4.18; found: C 64.53, H 7.58, N, 4.02.

2: ^{1}H NMR (500MHz, DMSO-$_{d6}$), δ 8.97-8.96 (d, *J* =5 Hz, 4H, Ar-H), 8.25-8.24 (d, *J* =5 Hz, 4H, Ar-H), 8.06-8.03 (d, *J* =15 Hz, 2H, vinyl-H), 7.84 (s, 4H, Ar-H), 7.63-7.60 (d, *J* =15 Hz, 2H, vinyl-H), 4.49-4.46 (t, 4H, N^{+}-CH_2), 1.89-1.87 (t, 4H, CH_2), 1.25-1.21 (m, 24H, CH_2), 0.83-0.81 (t, 6H, CH_3). ^{13}C NMR (100 MHz, CD_3OD): 155.18, 145.33, 141.81, 138.61, 130.10, 125.56, 125.28, 62.03, 32.92, 32.38, 30.47, 30.29, 30.13, 27.21, 23.70, 14.42. MALDI-TOF: m/z calcd for $C_{38}H_{54}N_2^{2+}$: 538.85; found: 539.205; elemental analysis calcd (%) for $C_{38}H_{54}N_2Br_2$: C 65.33, H 7.79, N 4.01; found: C 65.21, H 7.83, N, 4.07.

3: ^{1}H NMR (500MHz, DMSO-$_{d6}$), δ 8.97-8.95 (d, *J* =10 Hz, 4H, Ar-H), 8.24-8.23 (d, *J* =5 Hz, 4H, Ar-H), 8.05-8.02 (d, *J* =15 Hz, 2H, vinyl-H), 7.84 (s, 4H, Ar-H), 7.63-7.59 (d, *J* =20 Hz, 2H, vinyl-H), 4.49-4.46 (t, 4H, N^{+}-CH_2), 1.91-1.86 (t, 4H, CH_2), 1.25-1.21 (m, 28H, CH_2), 0.83-0.80 (t, 6H, CH_3). MALDI-TOF: m/z calcd for $C_{40}H_{58}N_2^{2+}$: 566.90; found: 567.451; elemental analysis calcd (%) for $C_{40}H_{58}N_2Br_2$: C 66.11, H 8.04, N 3.85; found: C 66.17, H 8.13, N, 3.71.

4: ^{1}H NMR (500MHz, DMSO-$_{d6}$), δ 8.97-8.96 (d, *J* =5 Hz, 4H, Ar-H), 8.25-8.23 (d, *J* =10 Hz, 4H, Ar-H), 8.06-8.03 (d, *J* =15 Hz, 2H, vinyl-H), 7.84 (s, 4H, Ar-H), 7.63-7.60 (d, *J* =15 Hz, 2H, vinyl-H), 4.49-4.46 (t, 4H, N^{+}-CH_2), 1.89-1.87 (t, 4H, CH_2), 1.26-1.21 (m, 16 H, CH_2), 0.84-0.81 (t, 6H, CH_3).. MALDI-TOF: m/z calcd for $C_{34}H_{46}N_2^{2+}$: 482.74; found: 481.934; Anal. Calcd for $C_{34}H_{46}N_2Br_2$: C 63.55, H 7.22, N 4.36; Found: C 63.68, H 7.16, N 4.42.

5: ^{1}H NMR (500MHz, DMSO-$_{d6}$), δ 7.82-7.81 (d, *J* =5 Hz, 4H, Ar-H), 7.40-7.39 (d, *J* = 5 Hz, 4H, Ar-H), 7.15 (s, 2H, vinyl-H), 4.84-4.82 (t, 4H, N^{+}-CH_2), 3.03-3.01 (m, 4H, N^{+}-CH_2-CH_2), 2.53-2.47 (m, 20H, CH_2), 2.19-2.17 (t, 6H, CH_3). MALDI-TOF: m/z calcd for $C_{28}H_{44}N_2^{2+}$: 408.66; found: 408.862; Anal. Calcd for $C_{28}H_{44}N_2Br_2$: C 59.16, H 7.80, N 4.93; Found: C 59.29, H 7.75, N 4.98.

6: ^{1}H NMR (500MHz, DMSO-$_{d6}$), δ 7.83-7.82 (d, *J* = 5 Hz, 4H, Ar-H), 7.40-7.39 (d, *J* = 5 Hz, 4H, Ar-H), 7.15 (s, 2H, vinyl-H), 4.84-4.82 (t, 4H, N^{+}-CH_2), 3.03-3.01 (m, 4H, N^{+}-CH_2-CH_2), 2.53-2.47 (m, 24H, CH_2), 2.19-2.17 (t, 6H, CH_3). MALDI-TOF: m/z calcd for $C_{30}H_{48}N_2^{2+}$: 436.71; found: 436.432; Anal. Calcd for $C_{30}H_{48}N_2Br_2$: C 60.40, H 8.11, N 4.70; Found: C 60.32, H 8.13, N 4.65.

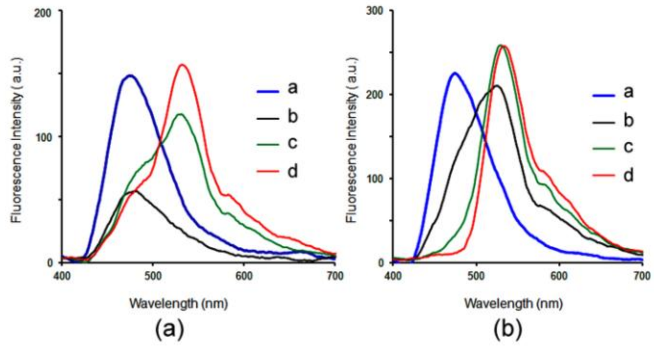

Figure S1. Fluorescence spectra changes of **1** (a) and **2** (b) with different concentrations in aqueous solution (a = 10 μM, b = 0.1 mM, c = 0.3 mM, d = 0.5 mM); λ_{ex} = 398 nm.

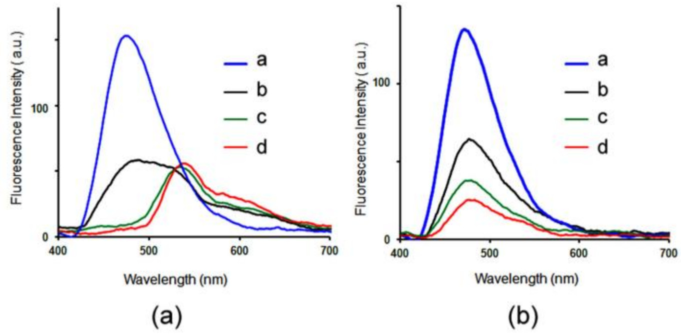

Figure S2. Fluorescence spectra changes of **3** (a) and **4** (b) with different concentrations in aqueous solution (a = 10 μM, b = 0.1 mM, c = 0.3 mM, d = 0.5 mM); λ_{ex} = 398 nm.

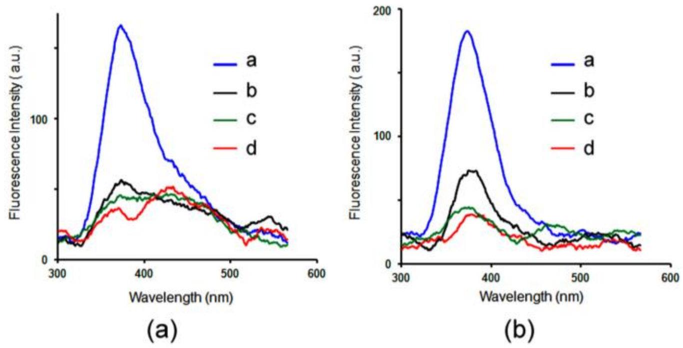

Figure S3. Fluorescence spectra changes of **5** (a) and **6** (b) with different concentrations in aqueous solution (a = 10 μM, b = 0.1 mM, c = 0.3 mM, d = 0.5 mM); λ_{ex} = 320 nm.

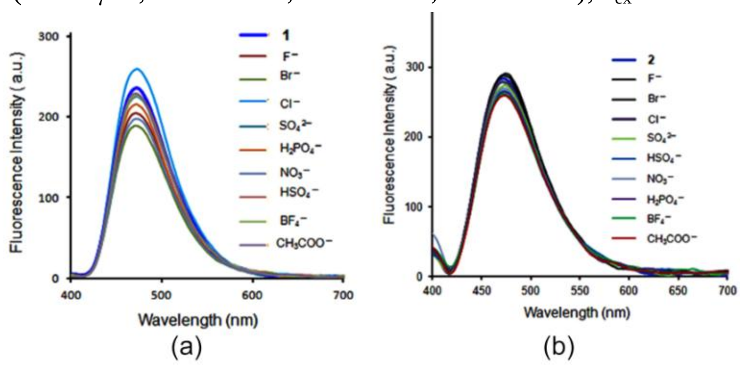

Figure S4. Fluorescence spectras of **1** (a) and **2 (b)** (each of 10 μM) with the addition of 20 equiv. of various anions as their tetrabutylammonium salts in aqueous solution at pH 7.4 (10 mM phosphate buffer). λ_{ex} = 398 nm.

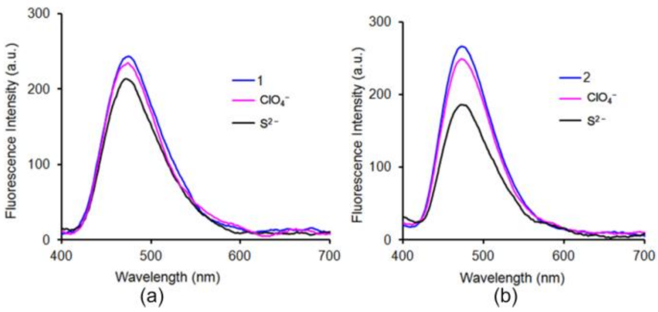

Figure S5. Fluorescence spectras of **1** (a) and **2** (b) (each of 10 μM) with the addition of 20 equiv. of ClO_4^- and S^{2-} as their sodium salts in aqueous solution at pH 7.4 (10 mM phosphate buffer). λ_{ex} = 398 nm.

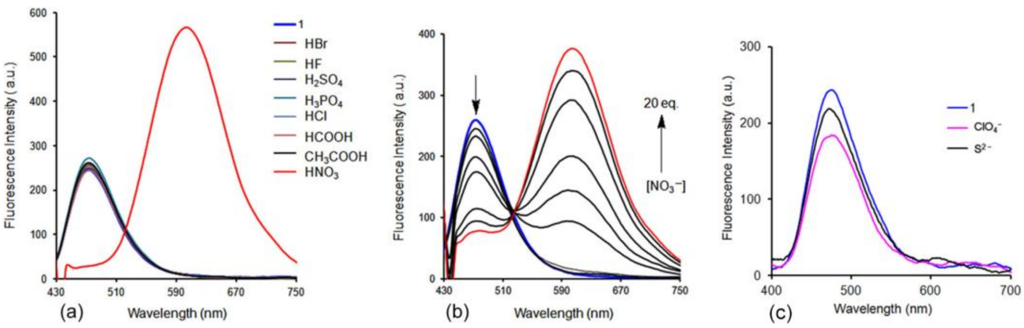

Figure S6. (a) Fluorescence response of **1** (10 μM) in aqueous solution with the addition of 20 equiv. of various acid species; (b) fluorescence spectra changes of **1** (10 μM) upon addition of increasing concentrations of NO_3^- (0−20 equiv.) as tetrabutylammonium salt in phosphate buffer solution (pH 6.0); (c) Fluorescence response of **1** (10 μM) in aqueous solution (pH≈4.0, 10 mM phosphate buffer) with the addition of 20 equiv. of ClO_4^- and S^{2-} as their sodium salts. λ_{ex} = 398 nm.

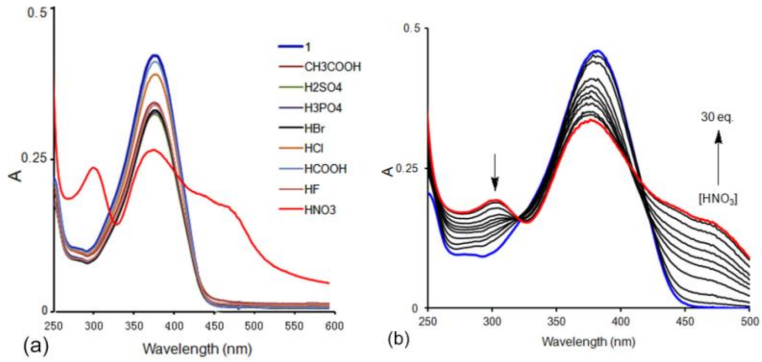

Figure S7. (a) UV-vis absorption spectra of **1** (10 μM) in aqueous solution with the addition of 30 equiv. of various acid species; (b) UV-vis absorption spectra changes of **1** (10 μM) upon addition of increasing concentrations of HNO_3 (0−30 equiv.) in aqueous solution.

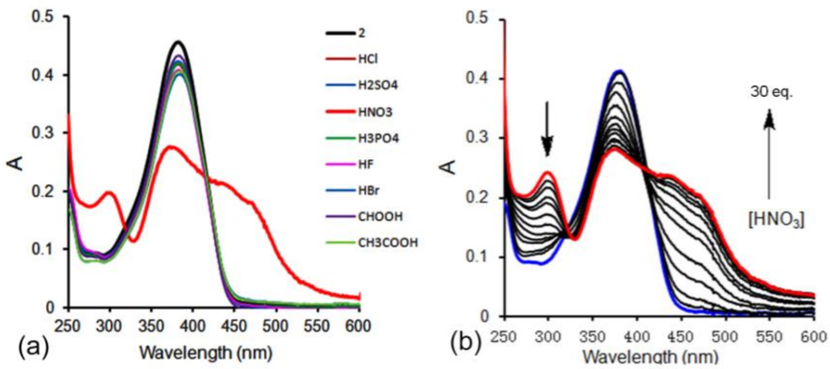

Figure S8. (a) UV-vis absorption spectra of **2** (10 μM) in aqueous solution with the addition of 30 equiv. of various acid species; (b) UV-vis absorption spectra changes of **2** (10 μM) upon addition of increasing concentrations of HNO_3 (0−30 equiv.) in aqueous solution.

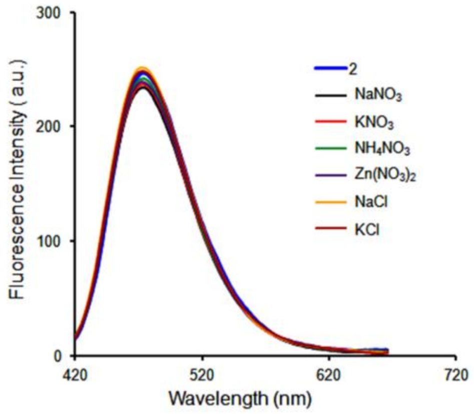

Figure S9. Fluorescence response of **2** (10 μM) in aqueous solution with the addition of 20 equiv. of various counter ions; λ_{ex} = 398 nm.

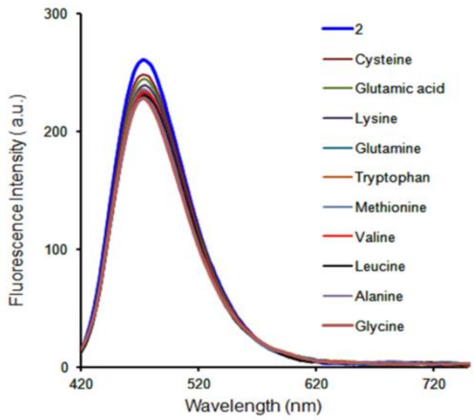

Figure S10. Fluorescence response of **2** (10 μM) in aqueous solution with the addition of 20 equiv. of various amino acids. λ_{ex} = 398 nm.

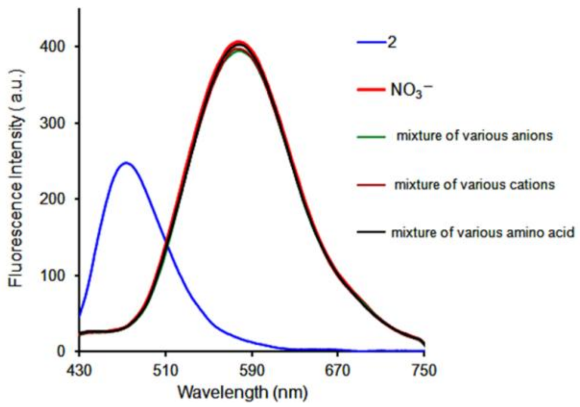

Figure S11. Fluorescence responses of **2** (10 μM) in phosphate buffer solution (pH 6.0) to various tested anions (mixture of Cl^-, SO_4^{2-}, HSO_4^-, $H_2PO_4^-$, Br^-, F^-, CH_3COO^-, ClO_4^- and S^{2-} each of 200 μM), cations (mixture of $NaNO_3$, KNO_3, NH_4NO_3, $Zn(NO_3)_2$, NaCl and KCl, each of 200 μM) and amino acids(mixture of cysteine, glutamic acid, lysine, glutamine, tryptophan, methionine, valine, leucine, alanine, glycine, each of 200 μM) in the presence of 200 μM NO_3^-.

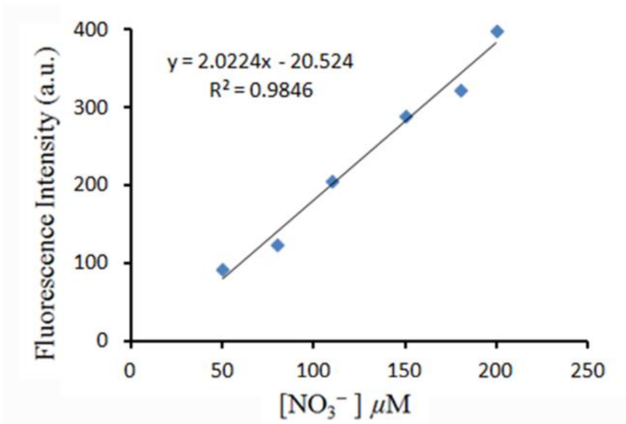

(a)

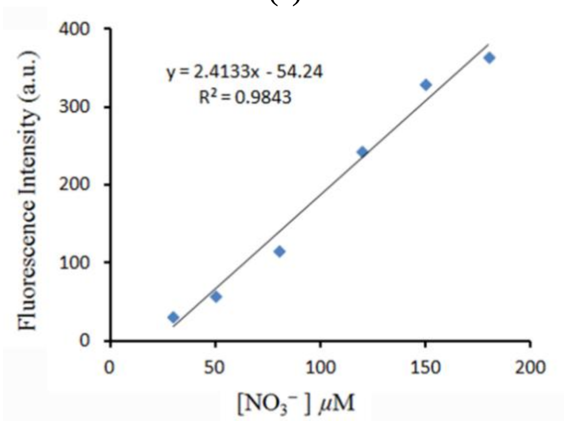

(b)

Figure S12. Plot of fluorescence intensity change (605 nm) of **1** (a) and **2** (b) with varied concentrations of NO_3^- at 298K, the limit of detection of NO_3^- was calculated to be 6.19×10^{-7} M for sensor **1** and 9.25×10^{-7} M for sensor **2**, respectively, by the formula (3σ/K).

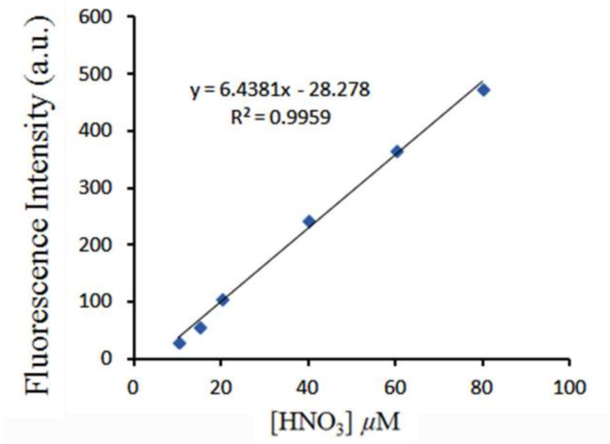

Figure S13. Plot of fluorescence intensity change (605 nm) of **2** with varied concentrations of HNO_3 at 298K, the limit of detection of HNO_3 was calculated to be 3.95×10^{-7} M by the formula ($3\sigma/K$).

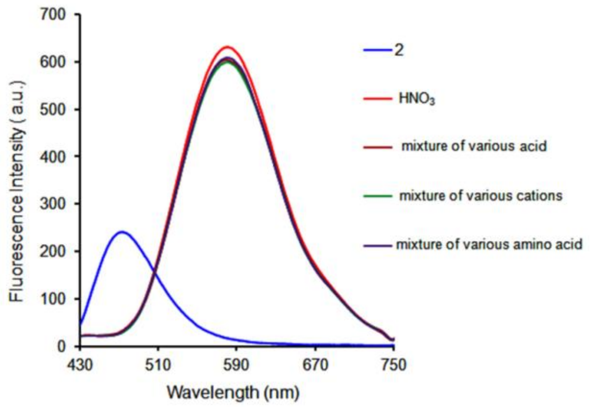

Figure S14. Fluorescence responses of **2** (10 μM) in aqueous solution to various tested acids (mixture of HCl, H_2SO_4, H_3PO_4, HBr, HF, CH_3COOH and HCOOH, each of 200 μM), cations (mixture of $NaNO_3$, KNO_3, NH_4NO_3, $Zn(NO_3)_2$, NaCl and KCl, each of 200 μM) and amino acids(mixture of cysteine, glutamic acid, lysine, glutamine, tryptophan, methionine, valine, leucine, alanine, glycine) in the presence of 200 μM HNO_3. λ_{ex} = 398 nm.

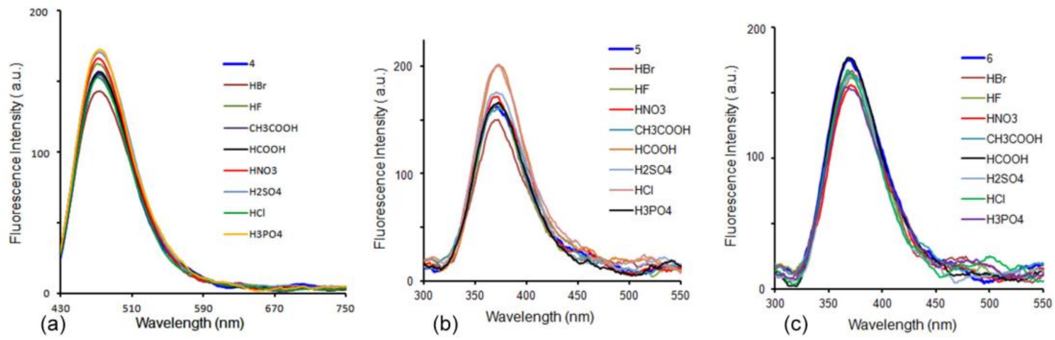

Figure S15. Fluorescence response of **4** (a), **5** (b) and **6** (c) (each of 10 μM) in aqueous solution with the addition of 20 equiv. of various acids.

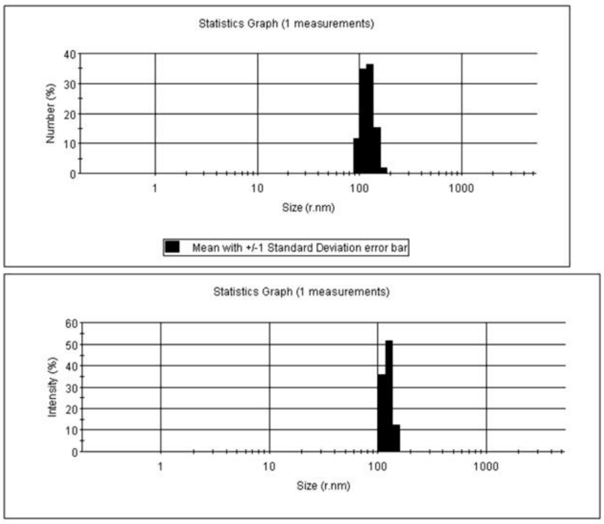

(a)

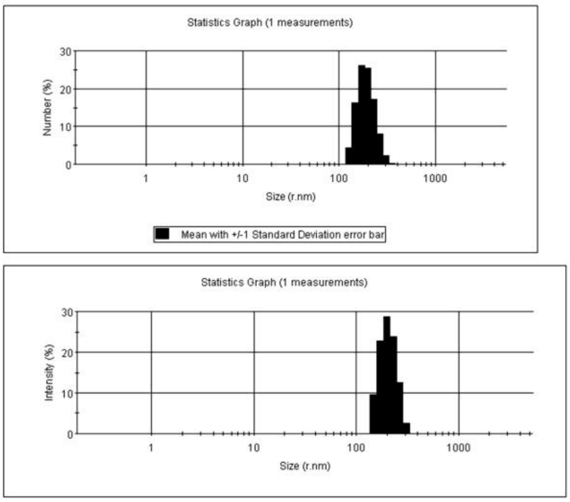

(b)

Figure S16. Distribution of hydrodynamic radii of aggregates of **1** (a) and **2** (b) (each of 10 μM) as measured through DLS at a scattering angle of 90^{o} after addition of addition of 20 equiv. of HNO_3 to the samples in aqueous solution.

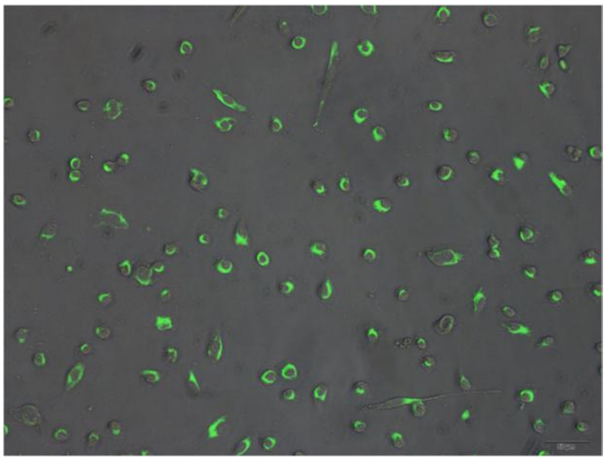

Figure S17. The overlay of fluorescence and bright-field images of DU145 cell lines incubated with **2** (5 μM) for 30 min at 37 ^{o}C**.**

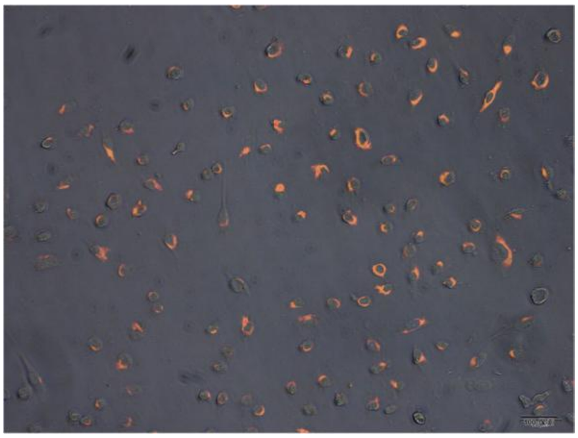

Figure S18. The overlay of fluorescence and bright-field images of DU145 cell lines incubated with **2** and then subsequently treated with KNO_3 (10 μM) and HNO_3 (10 μM) for 30 min at 37 ^oC.

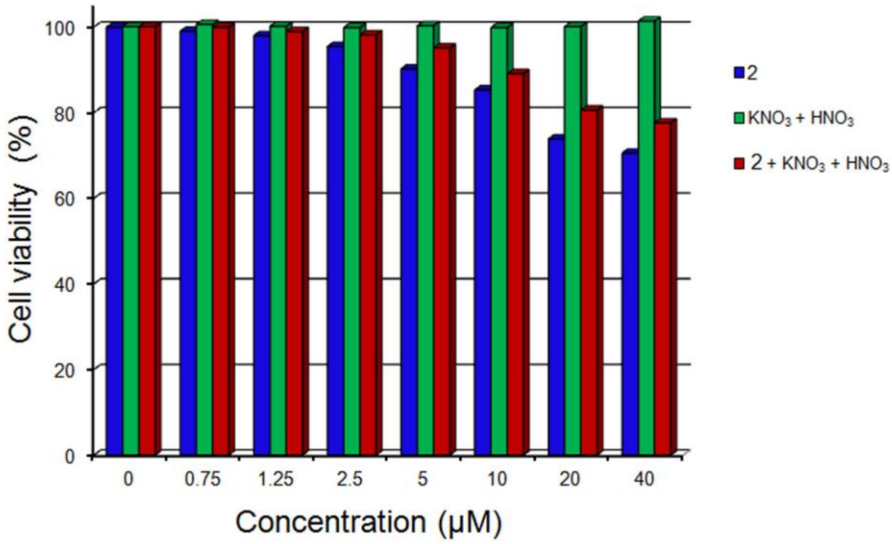

Figure S19. Percentage of DU145 cell viability remaining after cell treatment with **2**, KNO_3 and HNO_3, and **2** in the presence KNO_3 and HNO_3 (untreated cells were considered to have 100% survival). Cell viability was assayed by the MTT method (values: mean ± standard deviation).

References

1. Samanta, S. K.; Bhattacharya, S. *J. Mater. Chem*. **2012**, *22*, 25277–25287
2. Ichimura, K.; Watanabe, S. J. *J. Polym. Sci., Polym. Chem. Ed*. **1982**, *20*, 1419–1432.

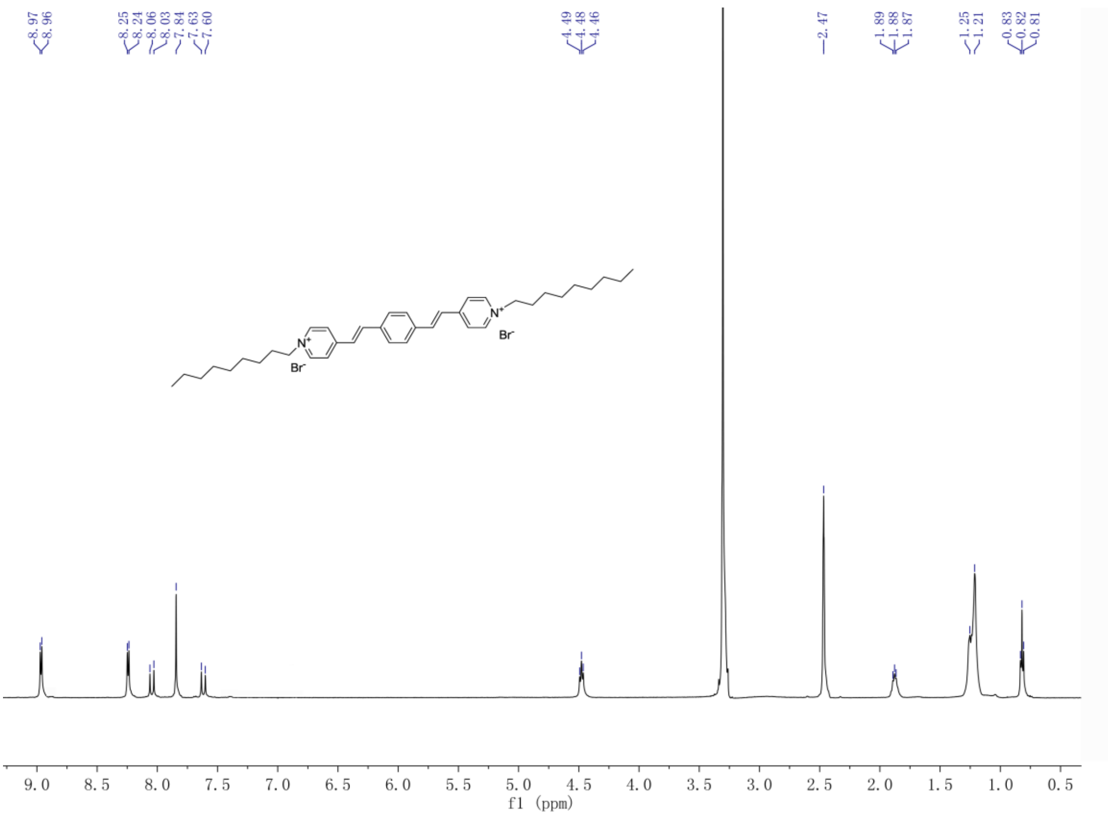

Figure S20. ^{1}H NMR spectra of **2** in DMSO-$_{d6}$

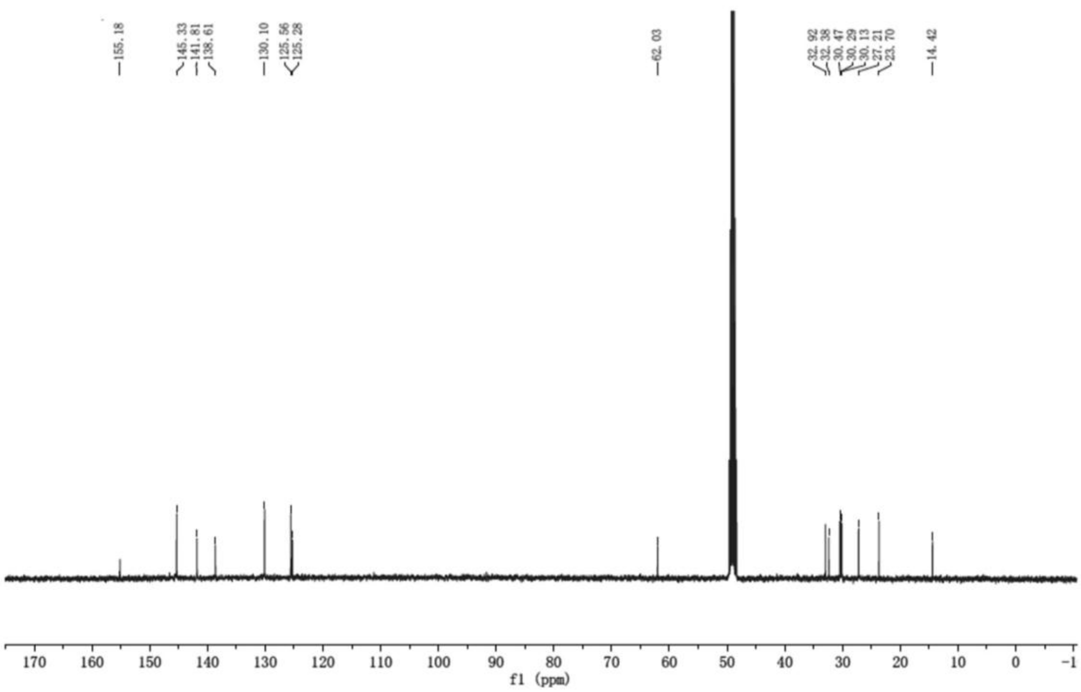

Figure S21. ^{13}C NMR spectra of **2** in CD_3OD

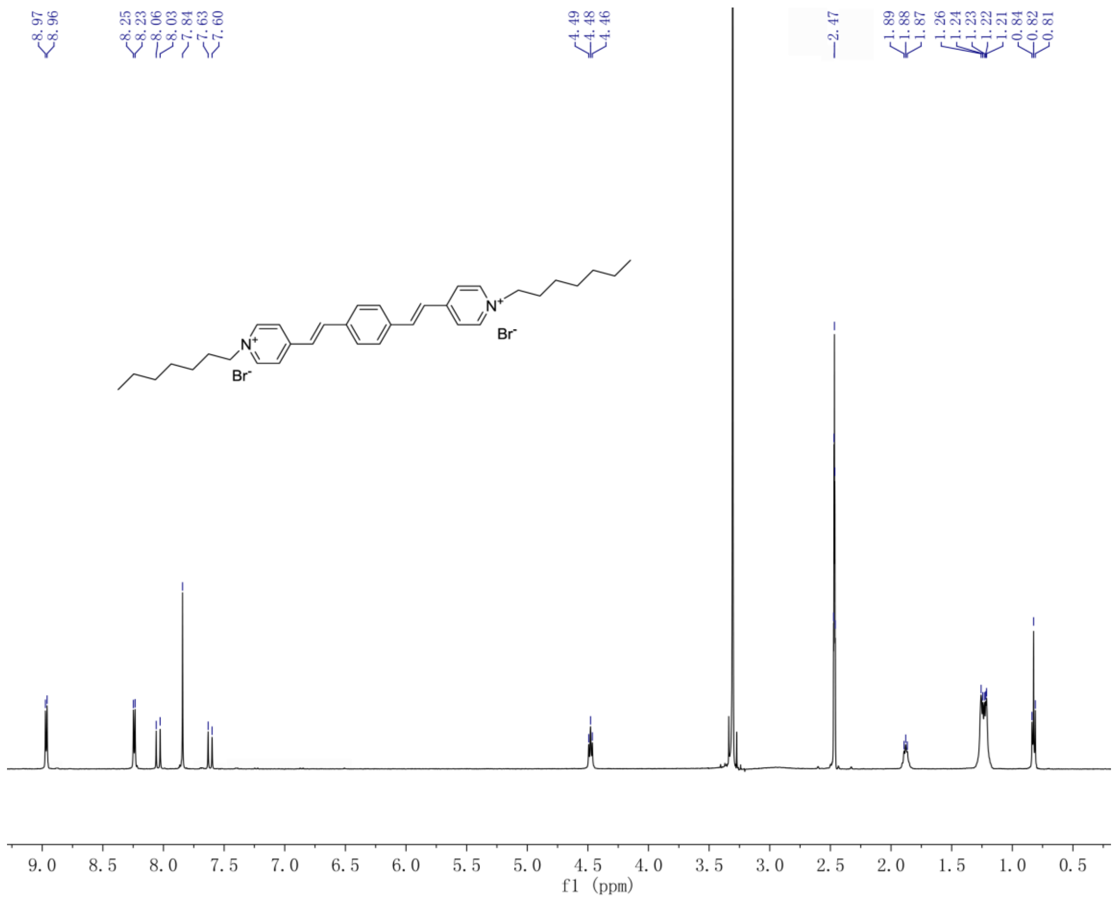

Figure S22. ^{1}H NMR spectra of **4** in DMSO-$_{d6}$

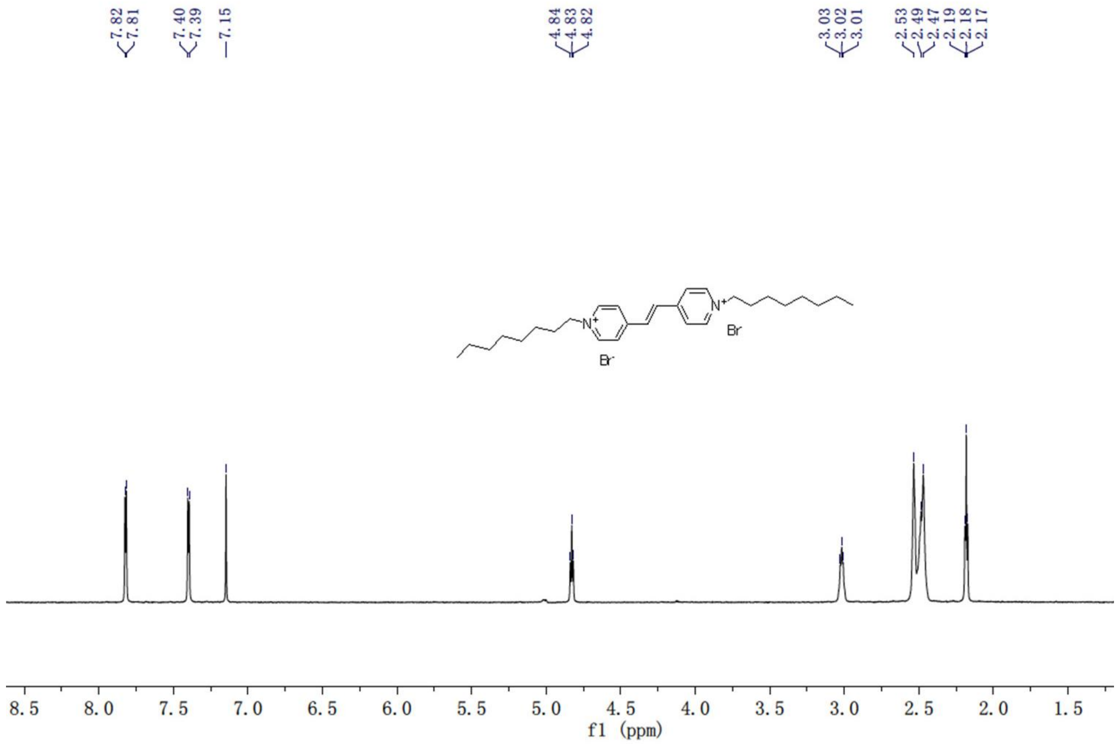

Figure S23. ^{1}H NMR spectra of **5** in DMSO-$_{d6}$

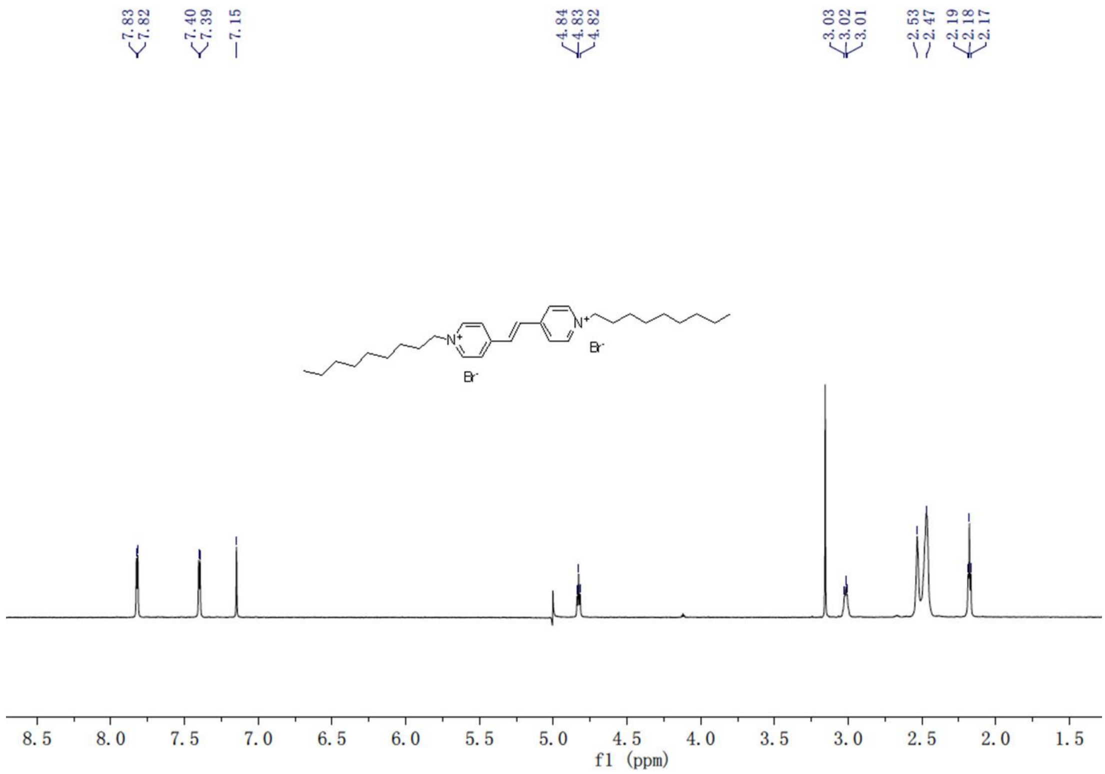

Figure S24. ^{1}H NMR spectra of **6** in DMSO-$_{d6}$